Electronic properties of Nb_3Ge and Nb_3Al from self-consistent pseudopotentials. II. Bonding, electronic charge distributions, and structural transformation

K. M. Ho, Warren E. Pickett,* and Marvin L. Cohen
Department of Physics, University of California and Materials and Molecular Research Division, Lawrence Berkeley Laboratory, Berkeley, California 94720
(Received 2 October 1978)

Electron charge distributions are presented for Nb_3Ge, Nb_3Al, and two hypothetical A-15 structures. Results indicate that the bonding in these materials is mainly metallic in character with some covalentlike bonding between Nb-chain atoms. We find significant coupling between neighboring chains and also between chain atoms and atoms at the cubic site. Comparison is made with various theoretical models. Investigation of the charge character of states near E_F suggests further developments in current theories on the structural transformation of A-15 compounds. The effect of chain dimerization on electronic states and charge distribution of Nb_3Ge is also investigated.

I. INTRODUCTION

We have recently performed self-consistent band-structure calculations for several A-15 compounds. A detailed description of the method of calculation, the electronic density of states, and the band-structure results has already been given in a previous paper,[1] hereafter denoted as I. In this paper, we will present the charge-density results for these compounds.

Band structures have been calculated for the A-15 compounds using the augmented-plane-wave method (APW)[2] and the linearized-muffin-tin-orbital method.[3] However, so far there have been no calculations of the electronic charge distributions in these compounds. We present in this paper calculated charge densities for Nb_3Ge and Nb_3Al based on the self-consistent-pseudopotential method.[4] The results for two other hypothetical A-15 "compounds" are also presented: One is Nb_3Nb, analogous to the β-tungsten phase, the other is one with Nb chains but with no atom at the cubuc B site, denoted as NB_3*. These systems have not been observed experimentally but are studied here with the hope of elucidating the effect of the B atom in the various properties of the A-15 compounds. Various theoretical models are discussed and compared with our results. Experimental data for charge distributions in A-15 compounds V_3Si and Cr_3Si are available from x-ray diffraction studies.[5] We will make some comparisons of our calculated charge distributions for Nb_3Ge and Nb_3Al with these results. In order to investigate the mechanisms leading to the structural instability in the A-15 structures we have also performed self-consistent calculations for a Nb_3Ge system in which one of the chains is dimerized.

Compounds crystallizing in the A-15 structure have the chemical formula A_3B, where A is a transition-metal atom and B may be a metal or a nonmetal. The crystal structure has the B atoms in a bcc sublattice with the A atoms in pairs on the cubic faces forming three sets of orthogonal chains (Fig. 1). These compounds have been studied intensively because of their high superconducting temperatures and unusual electronic and elastic properties.[6] Superconductors with the A-15 structure possess the highest superconducting transition temperatures (T_c) presently known. However, the reasons behind this high-T_c behavior are far from clear. Although many A-15 compounds have a high electronic density of states at the Fermi level [$N(E_F)$], this is not the only factor determining T_c. Specific-heat measurements[7] on several high-T_c A-15 compounds yield values of γ, the linear-term coefficient of the specific heat [which is proportional

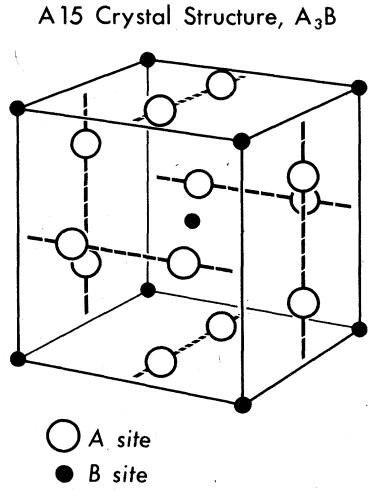

FIG. 1. Primitive unit cell for A-15 compound A_3B.

to $N(E_F)$] which do not correlate with the values of T_c. For example, Nb_3Ge has a γ value ~60% of that of Nb_3Sn, however, T_c for Nb_3Ge is higher than T_c of Nb_3Sn. Also elastic softening upon cooling has been observed in almost all high-T_c A-15 materials.[6] This indicates that variations in the electron-phonon coupling and the phonon frequency spectrum are also important factors in determining T_c.

Various theories have been used to try to explain high-T_c superconductors from the viewpoint of bonding characters and charge transfers. Hanke *et al.*[8] suggested that the hybridization of d states with nonmetallic p states near E_F in transition-metal compounds like carbides and nitrides can lead to enhancement in the electron-phonon coupling and phonon softening and hence higher T_c's. Vandenberg and Matthias[9] have observed that except for the rocksalt structure, crystal structures of high-T_c superconductors exhibit clustering of transition-metal atoms with long, but still metallic, intercluster separation. The combination of covalent intracluster and metallic intercluster bonding seems to be particularly favorable for high T_c. Pollak *et al.*[10] have attributed the large difference in T_c between crystalline and amorphous Nb_3Ge to the different bonding character in the two phases. Bongi[11] proposed a model describing the T_c variation of A-15 compounds in terms of a charge transfer between chain atoms and atoms in the cubic sites. Allen[12] has suggested that interchain charge transfer during atomic vibrations can result in soft TA modes leading to higher T_c. Thus knowledge of the charge density would enable us to further investigate the merits of the various theoretical models.

As mentioned in I, another interesting property of high-T_c A-15 compounds is that they undergo structural transitions at low temperatures.[13-18] The lattice experiences a cubic to tetragonal deformation and in the case of Nb_3Sn, a pairing up of the Nb atoms in two of the three sets of orthogonal chains was found to occur at the same time.[19] Models[20-24] have been proposed explaining the structural instability as being driven by an instability in the electronic spectrum through a Jahn-Teller or a Peierls mechanism. In particular Gor'kov[21] proposed a model which accounts for the structural transformation via a Peierls-like mechanism through the opening of a gap at X due to the sublattice distortion during the transformation (see Fig. 2). In the Gor'kov model, structural instability and superconductivity are linked together as being the result of the instability of the electronic spectrum at the X point against electron-electron and electron-phonon interactions, respectively. However, the Gor'kov model assumes a one-dimensional linear-chain band structure which subsequent band calculations[2] have shown to be unrealistic. Investigations have also been performed using phenomenological Landau-theory approaches[22,23] and group-theoretical methods.[24]

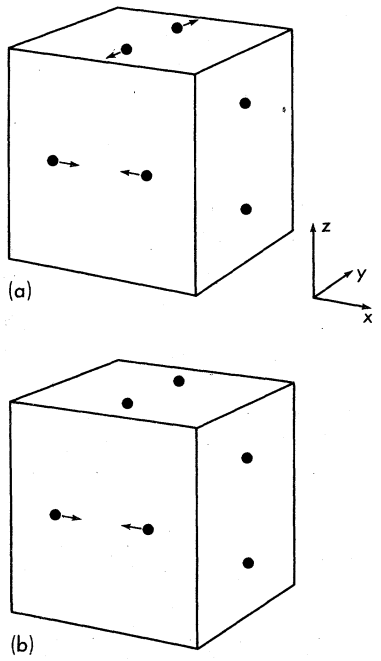

FIG. 2. (a) Sublattice distortion of Nb_3Sn during structural transformation from neutron-diffraction data; (b) dimerization of Nb_3Ge used in present calculation.

II. CALCULATION

Since a detailed discussion of our method of calculation is given in paper I, we will only give a brief description here. Our results were obtained by a self-consistent-pseudopotential technique which has been applied successfully to band-structure calculations of a wide variety of materials including semiconductor and transition-metal bulk and surfaces. A mixed basis approach[4] was employed in the present calculation: in addition to the usual plane waves, a set of localized orbitals was also included in the basis in solving the crystal Hamiltonian to ensure sufficient convergence for the d states. This approach has been proved successful in calculations of the properties of transition-metal bulk[4] and surfaces.[25] The crystal charge densities were expanded using ~2100 plane waves corresponding to a cutoff energy of ~25.7 Ry. The self-consistent valence charge densities for Nb_3Ge and Nb_3Al were calculated using a weighted aver-

age of 14 $\vec{k}$ points in the irreducible Brillouin zone whereas for Nb_3Nb and Nb_3^*, only 4 $\vec{k}$ points were used. The differences between the results for 4 $\vec{k}$ points and 14 $\vec{k}$ points are very small for Nb_3Ge and Nb_3Al.

III. RESULTS

A. Total valence charge distributions for Nb_3Ge and Nb_3Al

In Fig. 3 we present contour plots of the total valence charge distributions of Nb_3Ge and Nb_3Al on a face of the cubic unit cell containing a niobium chain. The contours are in units of electrons per unit cell. These plots give the valence electron charge density based on pseudo-wave-functions. The charge of the core electrons is not included and we have not orthogonalized the valence electron pseudo-wave-functions to the core atomic wave functions. Thus, our charge densities or pseudocharge densities are accurate only for regions outside the cores of the atoms. The charge distributions for the two materials are very similar. The most prominent feature is a pile up of the d electrons along the niobium chains forming a "double hump" between atoms on the chains. This is superimposed on a smooth charge background in the interstitial regions. The magnitudes and positions of the "double hump" are almost identical for Nb_3Ge and Nb_3Al. The charge density between the chain atoms is slightly higher in Nb_3Ge probably due to the shorter interatomic distances in Nb_3Ge. (The cubic-unit-cell length $a_{Nb_3Ge}=5.166$ Å while $a_{Nb_3Al}=5.187$ Å.) The main difference is that the Ge atom retains one more electron in Nb_3Ge than does Al in Nb_3Al.

In order to investigate the bonding and charge transfer we compare the total valence charge densities of Nb_3Ge with that obtained by overlapping spherical Nb and Ge atomic charge densities. In Fig. 4 we have contour plots of the charge-density *difference* between A-15 Nb_3Ge and overlapping spherical atoms. The plot is on a cubic face passing through a niobium chain. The difference is negative around both atoms and positive in the interstitial regions: charge is taken from the atoms, especially from regions around the niobium atoms, and spread out all over the unit cell enhancing the metallic characteristics of the crystal. We also notice a charge buildup along the chains; this indicates the presence of covalentlike bonding between neighboring atoms on the chain. However, the charge buildup along the chain is smaller in magnitude than the charge flow to the interstitial regions. We conclude that bonding in Nb_3Ge is mainly metallic in character with some covalentlike bonding between neighboring niobium atoms on a chain. From the charge-density difference plots, we also see a slight increase of charge in the region (not shown) between neighboring chains indicating an interchain coupling. The case of Nb_3Al is similar and will therefore not be discussed.

B. Charge transfer

Bongi[11] has proposed a model describing the variation of T_c among A-15 alloys by postulating a charge transfer between the atoms in the cubic site and the atoms in the chain sites which is proportional to the difference Δn_{ws} of the density of electrons at the limits of the Wigner-Seitz cell of the two kinds of atoms. Using this model, he concluded that in Nb_3Ge, 1.35 electrons

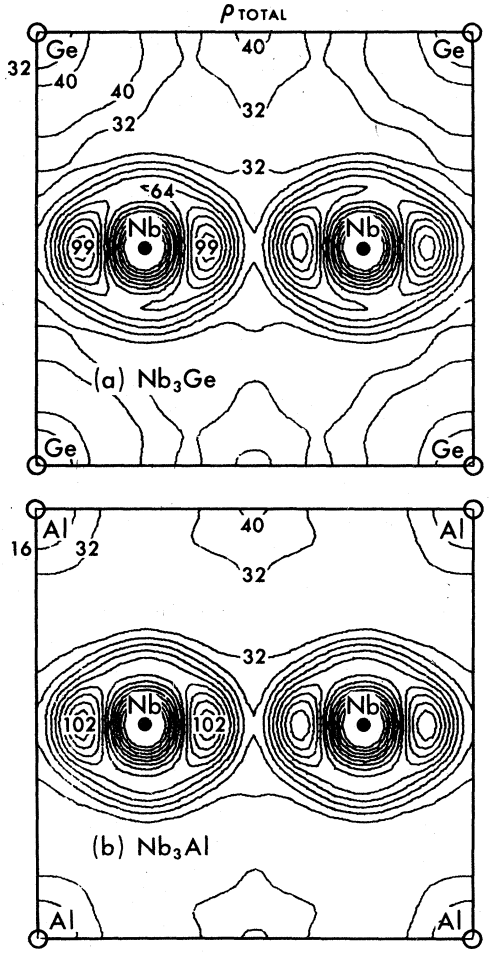

FIG. 3. Contour plots of the total valence charge distributions of (a) Nb_3Ge, (b) Nb_3Al on face of cubic unit cell. Contour labels are in units of number of electrons per unit cell. Position of atoms in the plane are indicated by filled and open circles. Contours are in steps of eight units.

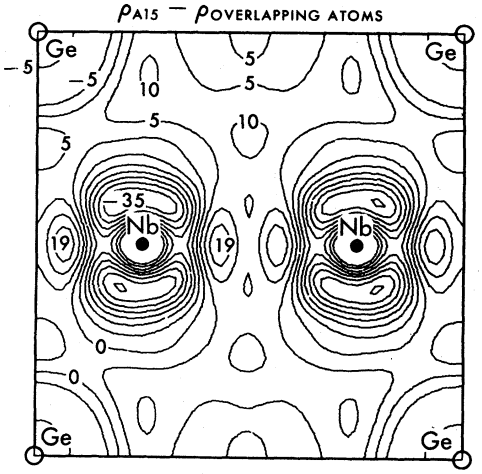

FIG. 4. Contour plots of the difference between the total charge density in crystalline Nb_3Ge and charge density due to overlapping spherical Nb and Ge atoms on a face of the cubic unit cell. Contours are in steps of 5 electrons per unit cell.

are transferred from each Ge atom to the Nb atoms and in Nb_3Al 0.84 electrons are transferred from each Al atom to the Nb atoms. In order to investigate the charge transfer in the system we have partitioned the unit cell into various regions and computed the charge in these regions for Nb_3Ge. The results are listed in Table I. The values for overlapping spherical atoms are also listed. We find no evidence for increase of charge around the Nb atoms in contrast to Bongi's ionic picture. In view of the high anisotropy and the presence of covalent behavior in the A-15 structure, we question Bongi's extension of Miedema's approach.[26] Another point to be made is that it is not clear that the Δn_{WS} values between constituent atoms can be interpreted in terms of a charge transfer between the atoms in A-15 compounds. For example, Bongi predicted more charge will be transferred away from the Ge atoms than from the Al atoms; this conflicts with our calculated results and is contrary to simple considerations of the electronegativities of the two elements.

Actually, in a metallic compound with inequivalent atomic sites it is impossible to define the "charge transfer" in an unambiguous way since the metallic charge density in the interstitial region cannot be assigned straightforwardly to a particular atom. This problem has been discussed at some length by Staudenmann *et al.*,[5] who have published experimental results for the charge densities of the A-15 compounds V_3Si and Cr_3Si. For V_3Si, which is isoelectronic with Nb_3Ge, they suggested a "charge transfer" of 1.8–2.4 electrons from the silicon to the vanadium atoms. However, this result involved assigning most of the interstitial charge density to the V atoms in a rather arbitrary manner. If one takes the conventional Wigner-Seitz cells to define the regions of integration for the experimental charge densities one would have obtained a vanishing "charge transfer." We suggest that the above results, like ours, can be most realistically interpreted in a metallic-bonding picture. Staudenmann *et al.*[5] also reported a pile up of charge along the chains similar to our calculated results for the Nb-based A-15 compounds. However, no "double-hump" structure is observed along the chains in the V_3Si data. Since vanadium is in the third row of the Periodic Table, the d electrons are much more localized in vanadium than in niobium. (In the atom, the d wave function peaks at 0.85 and 1.4 a.u. for vanadium and niobium, respectively.) Thus the "double-hump" structure would be expected to be nearer the core and much smaller in magnitude. The problems associated with core subtraction could account for this structure not being observed. Also the plane-wave expansion of the experimental charge density was cut off at about 16 Ry; truncation of high Fourier components would cause a smoothing out of sharp structures.

TABLE I. Results of partitioning of charge in Nb_3Ge (in units of number of electrons per atom); a_c is the length of the cubic unit cell.

	A-15	Overlapping atoms
For Nb		
Muffin-tin sphere, radius $\frac{1}{4}a_c$	3.11	3.49
Wigner-Seitz cell	4.79	4.92
Cylinder around chain, radius $\frac{1}{4}a_c$	4.09	4.31
For Ge		
"Touching" muffin-tin sphere, radius $=[(\sqrt{5}-1)/4]a_c$	4.68	4.33
Wigner-Seitz cell	4.63	4.24
Muffin-tin sphere, radius $=r_{Ge}=1.22$ Å	2.33	2.44

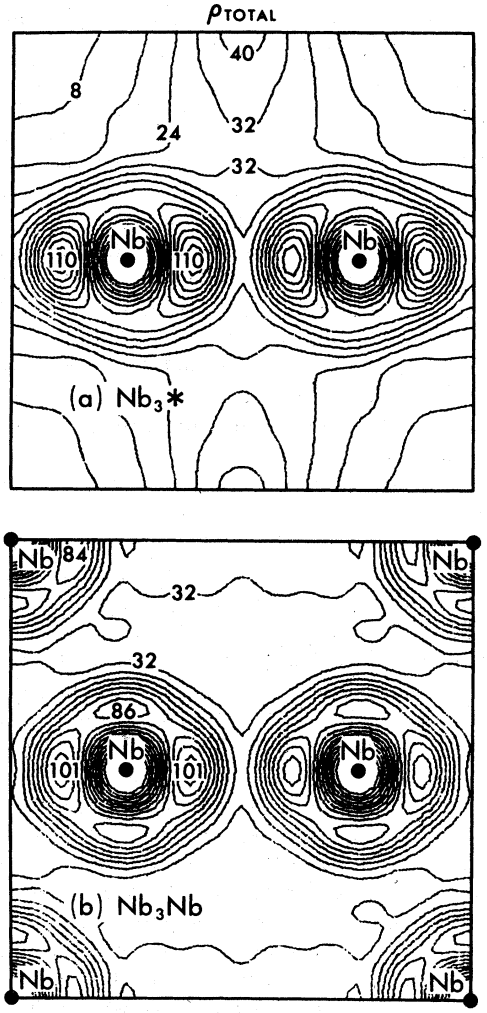

FIG. 5. Contour plots of the total valence charge distributions of (a) Nb_3^*, (b) Nb_3Nb on face of cubic unit cell, in units of electrons per unit cell.

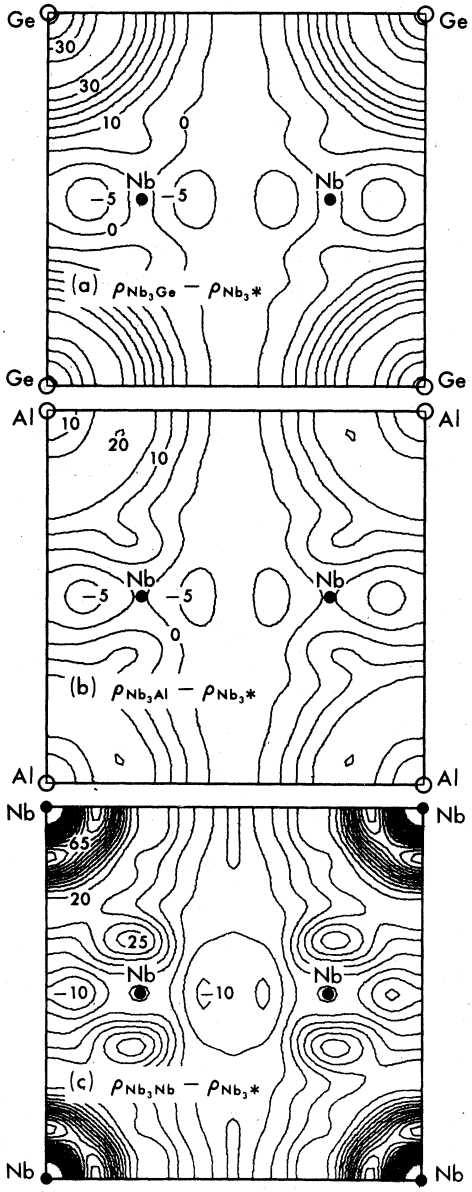

FIG. 6. Contour plots of the difference between the charge densities of (a) Nb_3Ge, (b) Nb_3Al, (c) Nb_3Nb and the charge density of Nb_3^*. Contours are labeled in units of electrons per unit cell.

C. Nb_3Nb and Nb_3^*

In order to investigate the effect of the cubic-site atom on the niobium chains, we have calculated the charge densities for two hypothetical A-15 compounds: Nb_3^*, which has vacant cubic sites, and Nb_3Nb, which has Nb atoms in the cubic site. The cell dimension for Nb_3^* was chosen to be the same as that of Nb_3Ge while for Nb_3Nb we use a value of 5.26 Å as suggested by previous works.[27] In Fig. 5, we have plotted the total valence charge distribution for Nb_3^* and Nb_3Nb on the same plane as in Fig. 3. In Nb_3^*, the charge is less metallic and located more densely along the chains. The interchain coupling is also stronger than in the cases where the cubic site is occupied. In Nb_3Nb, the "double-hump" structure, although present, is comparatively weaker, since charge also is moved to lobes perpendicular to the chain. There is almost no coupling between neighboring chains. In Fig. 6, we have plotted difference charge densities of $\rho_{Nb_3Ge} - \rho_{Nb_3^*}$, $\rho_{Nb_3Al} - \rho_{Nb_3^*}$, $\rho_{Nb_3Nb} - \rho_{Nb_3^*}$ (neglecting the small differences in the dimension of the unit cells). Putting an atom in the cubic site has the effect of weakening the bonding between neighboring Nb atoms on a chain and also the

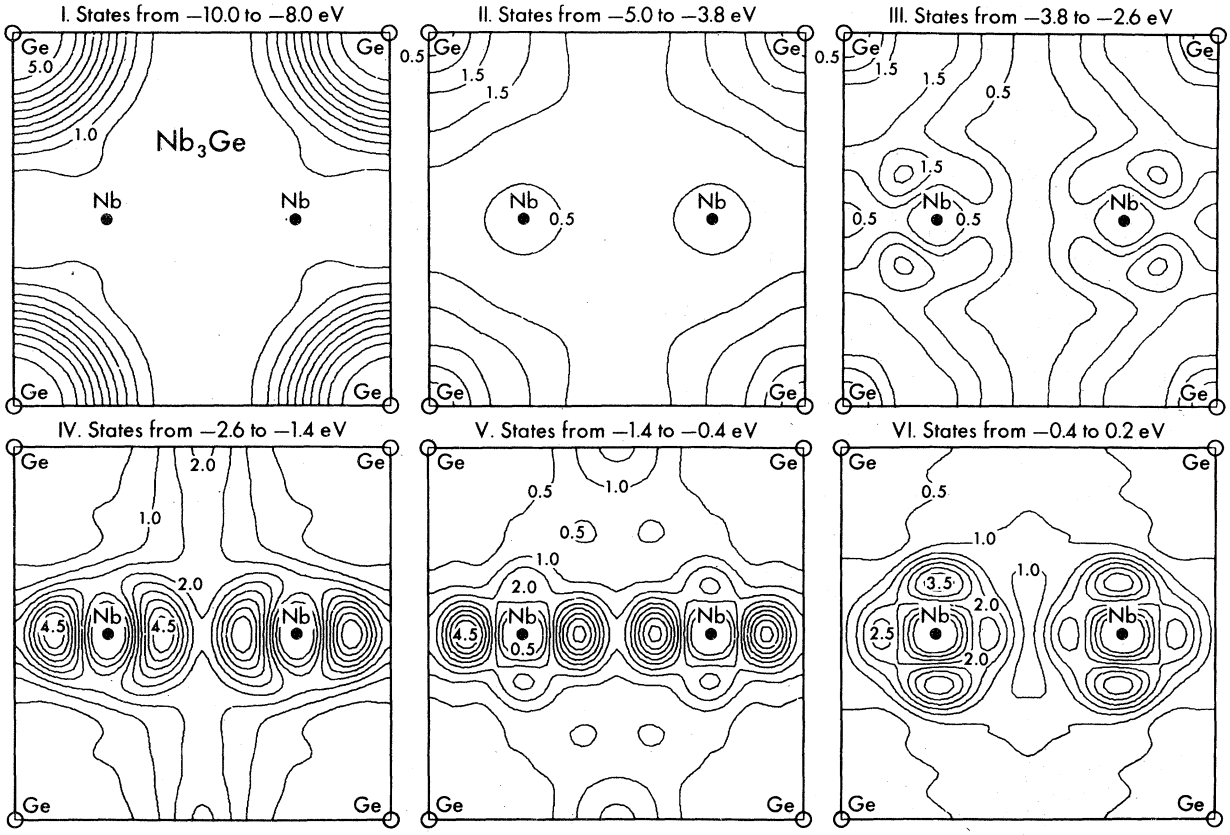

FIG. 7. Charge distribution of states of Nb_3Ge in different energy regions: I, −10.0 to −8.0 eV; II, −5.0 to −3.8 eV; III, −3.8 to −2.6 eV; IV, −2.6 to −1.4 eV; V, −1.4 to −0.4 eV; and VI, −0.4 to 0.2 eV. All the charges are normalized to one electron per unit cell.

coupling between neighboring chains. This is accompanied by the development of a pile up of charge between the cubic-site atom and the neighboring chain atoms, indicative of covalent bonding between these atoms. The effect is small in Nb_3Ge and Nb_3Al, but becomes very pronounced in Nb_3Nb. This weakening of chain behavior and the development of bonding between the d states might be the cause of the very different properties of A-15 compounds with transition metals in the cubic site and those with nontransition metals in the cubic site.

D. Charge in various energy regions

In Fig. 7, we have plotted the charge densities of states of Nb_3Ge in different energy regions under various peaks in the electronic density of states.[1] The energy ranges for the different regions are given with respect to the Fermi level as follows: region I, −10 to −8 eV; region II, −5.0 to −3.8 eV; region III, −3.8 to −2.6 eV; region IV, −2.6 to −1.4 eV; region V, −1.4 to −0.4 eV; and region VI, −0.4 to 0.2 eV. Region I is composed of Ge s states which are split off from the rest of the bands. Region II is mainly Ge p states. In region III we have a bonding mixture of Ge p states with the Nb d_{xz}, d_{yz} (taking the chain direction as the z axis) states along the chain. Regions IV, V and VI are mainly composed of states associated with the Nb chains. In region IV, the charge is heavily $d_{3z^2-r^2}$-like along the chains with strong interactions between neighboring Nb atoms and neighboring chains. The charge in this region resembles the charge distributions for the Nb_3^* system. The charge in region V in addition to lobes along the chain has lobes pointing perpendicular to the chain indicating a mixing in of $d_{x^2-y^2}$ states. Investigation of the charge distribution in the plane perpendicular to the chain reveals a large d_{xy} character in the charge. In region VI, the states are mainly $d_{x^2-y^2}$ like with mixing in of some $d_{3z^2-r^2}$ character. Above region VI, we have mainly antibonding d states from the Nb atoms.

E. States near E_F

In Fig. 8 we have plotted the charge distributions for states which are less than 0.1 eV below the Fermi level for Nb_3Ge and Nb_3Al. We can see that the character of the states near E_F are quite similar in the two compounds. In both compounds, we have a mixture of $d_{x^2-y^2}$ and $d_{3z^2-r^2}$ types of states. The Nb_3Ge states near E_F have more $d_{3z^2-r^2}$ character than states near E_F in Nb_3Al. Bhatt[23] has recently constructed a model for A-15 compounds in which he assumed that states near E_F have a $d_{x^2-y^2}$ character. In our results, although states near E_F have a strong $d_{x^2-y^2}$ character, there are significant mixtures of $d_{3z^2-r^2}$ character which might also play a role in the various properties of these compounds, particularly in Nb_3Ge. In both compounds, we notice a charge increase in the regions between the chains and the cubic site indicating a hybridization of the chain d states with the p states at the cubic site. This effect is more pronounced for Nb_3Ge than for Nb_3Al. In their studies on transition-metal compounds such as carbides and nitrides, Hanke *et al.*[8] have suggested that hybridization of the transition-metal d states with nonmetallic p states leads to the building up of bonding charges which can increase T_c through the softening of phonons and a resonant enhancement in the electron-phonon coupling due to the added screening. This mechanism appears to be partly responsible for the high T_c in A-15 compounds although the exact magnitude of this enhancement remains to be calculated.

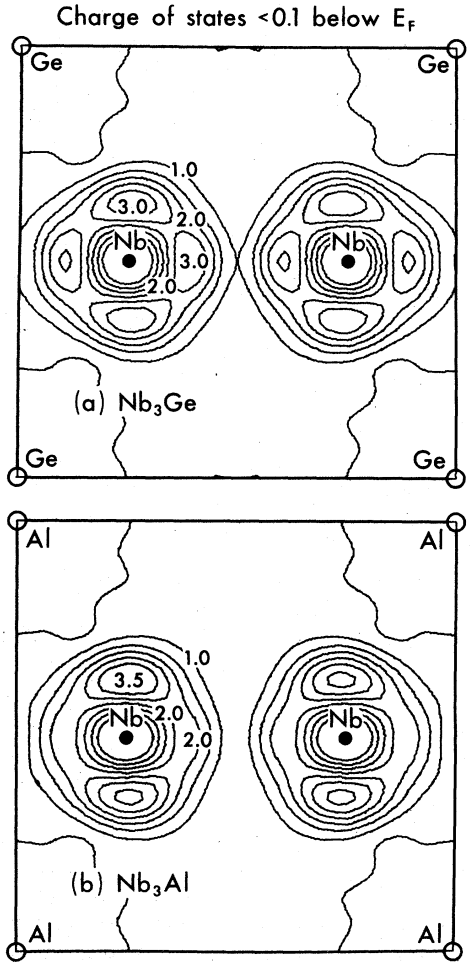

FIG. 8. Charge distributions of states less than 0.1 eV below Fermi level of (a) Nb_3Ge and (b) Nb_3Al. The charge distributions are normalized to one electron per unit cell.

In Fig. 9, we have plotted the charge densities for individual states near E_F at several symmetry points in the Brillouin zone. In Nb_3Al, the Fermi level passes very near a fourfold degenerate level $R_{1,2}$ at R while in Nb_3Ge the Fermi level lies almost right on top of the sixfold degenerate R_4 state.[1] Other states plotted are Γ_{12}, M_9, X_1 all of which are doubly degenerate. The energies of these states with respect to the Fermi level are, in units of eV: Γ_{12}, 0.03; X_1, −0.37; M_9, −0.06; R_4, −0.00; $R_{1,2}$, −0.12 for Nb_3Ge; and Γ_{12}, 0.02; X_1, −0.31; M_9, 0.05; R_4, 0.12; $R_{1,2}$, −0.02 for Nb_3Al. The charge densities plotted are for Nb_3Ge, but since these states are essentially d states from the Nb, their charge distributions are quite similar in Nb_3Al. We can see that the charge for the states Γ_{12} and X_1 have charge distributions which are mostly concentrated in lobes perpendicular to the chains whereas the states at M and R have charge located more densely between the chains. This has important implications for various models on the structural transformation of A-15 compounds. In the event of a structural transformation where the chains are distorted, one would expect the states at Γ and X to be relatively unaffected while states at R and M would play a more active role.

F. Dimerization

Various models[20-23] have been proposed for the structural transformation of high-T_c A-15 compounds based on the assumption that the splitting of degenerate states at symmetry points near the Fermi level due to the distortion of the lattice could lead to a Peierls-type instability or to a band Jahn-Teller effect. A popular model is the Gor'kov model[21] where it is assumed that the Fermi level passes through a doubly degenerate level at the point X which is split by a chain dimerization via a Peierls-type mechanism, causing an instability

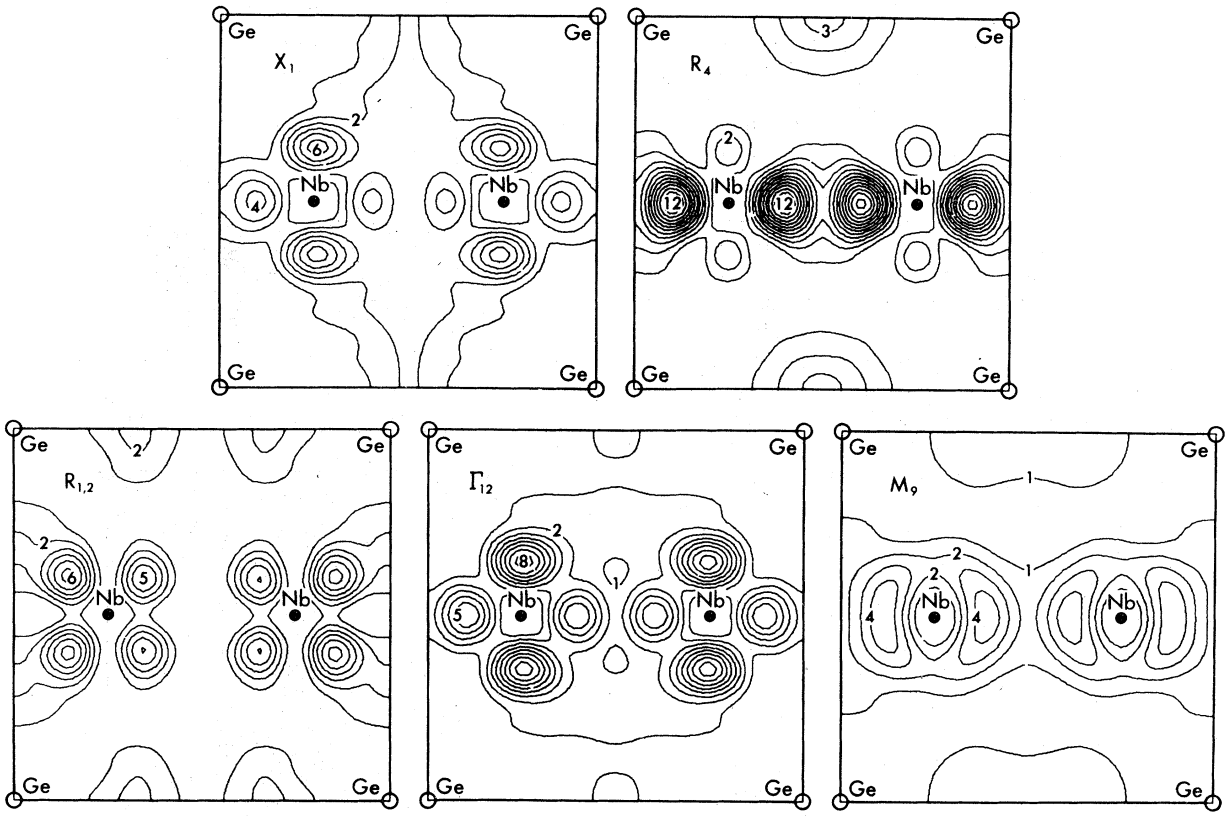

FIG. 9. Charge densities of individual states near E_F at Γ $[(0,0,0)]$, X $[(\pi/a_c,0,0)]$, M $[(\pi/a_c,\pi/a_c,0)]$, and R $[(\pi/a_c, \pi/a_c,\pi/a_c)]$ for Nb_3Ge. The charge for each state is normalized to one electron per unit cell.

in the electronic spectrum which is the driving force of the structural transformation. Since the introduction of this model, various investigations[22,23,28] on the structural transformation of A-15 compounds have followed this assumption.

To better understand the mechanisms leading to the structural instability in the A-15 structure,

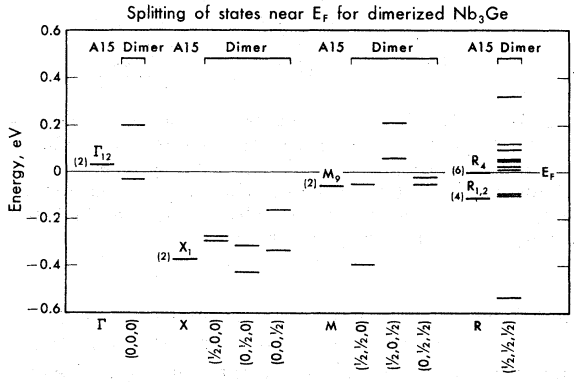

FIG. 10. Schematic diagram showing splitting of states near E_F at Γ, X, M, and R as a result of dimerization of the x chain in Nb_3Ge. The Fermi levels of the dimerized and undimerized system have been lined up.

we have performed self-consistent calculations for a Nb_3Ge system in which one of the three sets of orthogonal chains is dimerized. The Nb atomic displacements in the dimerized chain is 1.5% of the unit-cell length, which is about 5 times the experimentally observed values of Nb_3Sn.[19] The larger value was chosen so that effects due to the dimerization would not be masked by the noise in the calculations coming from self-consistency procedures.

In Fig. 10, we have shown the splitting of the levels at various symmetry points arising from the dimerization. It can be seen that the states most affected are the ones at R and M, where splittings of the order of 1 and 0.6 eV, respectively, are observed. The splittings at Γ and X are quite small (~0.2 eV) compared with those at R and M. From our results, it appears more reasonable that any theory proposing a Peierls or Jahn-Teller type of electronic instability should consider the R and M points (particularly the R point) rather than Γ or X points in the Brillouin zone. Recently Lee *et al.*[29] have noted that a $\vec{k}\cdot\vec{p}$ expansion around the R_4 point can lead to a peak in the density of states. These authors have

applied this model to Nb_3Sn and V_3Si to explain the anomalous temperature dependence of the susceptibility and elastic properties. However, in Nb_3Al we find that E_F does not lie close to the R_4 state and for Nb_3Ge, an attempt to fit the model parameters to our band structure revealed that the $\vec{k} \cdot \vec{p}$ expansion is only valid for less than 10^{-6} of the volume of the Brillouin zone, presumably due to the close proximity of the $R_{1,2}$ level which is neglected in the $\vec{k} \cdot \vec{p}$ models.

Rather unexpectedly, the splitting of the R_4 states with dimerization is much less than that of the $R_{1,2}$ and M_9 states. Comparing the charge distributions for Γ_{12}, X_1, R_4 and those for the $R_{1,2}$ and M_9 states, we see the latter pair of states which are split most have *larger interactions with the cubic-site atom* than the other states. Thus the interaction of the Nb chain with the Ge atoms is very sensitive to displacements of the Nb atoms. This would seem to tie in with the ideas of Pollak *et al.*[10] who proposed that the difference in T_c in amorphous and crystalline Nb_3Ge is caused by the different character of the bonding due to a change in the interaction of the Nb and Ge atoms in going from the crystalline to the amorphous phase.

In Fig. 11, we present the charge distributions of our dimerized Nb_3Ge system on the three cubic faces which are now inequivalent because of the symmetry change. The top figure shows the charge distribution on the x-z plane which contains the dimerized chain (the x chain). The main effect of the dimerization is a *transfer of charge along the chain*. The charge density in the region where the chain atoms come together increases by ~30% whereas at the place where the chain atoms come apart, the charge density decreases by ~20%. The changes in the other two chains are small. In Fig. 12, we have plotted the difference between the charge densities of the dimerized system and the original Nb_3Ge system on the x-z plane which contains the dimerized chain. The two lobes, one positive and one negative around the Nb atoms, reflect the rigid shift of the d states with the atoms. The main feature is a piling up of charge in the center at the expense of a depletion of charge from the region where the atoms move apart. The charge differences in the other parts of the cell are small.

To investigate any possible charge transfer we have calculated the charge on each of the three chains by summing up the contributions from cylinders around each chain with radii $\frac{1}{4}a_c$. The results are given in Table II together with the corresponding results for the undistorted Nb_3Ge system. It can be seen that the charge flow occurs mainly within the dimerized chain

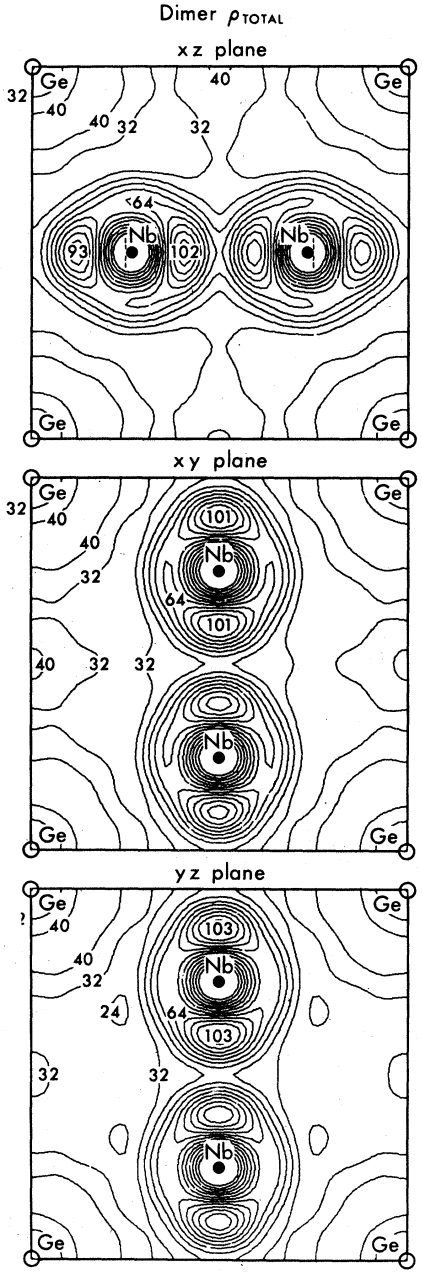

FIG. 11. Total valence charge distributions of the dimerized Nb_3Ge system on the three faces of the cubic unit cell. (a) Displays the charge distributions for the dimerized chain (the x chain). The charge densities are in units of electrons per unit cell. The dashes indicate the position of the unshifted Nb atoms.

and there is little interchain transfer. A large part of the differences comes from the noise in the calculation coming from the self-consistency procedure. However, these results do not rule out charge transfer arising from the tetragonal deformation.

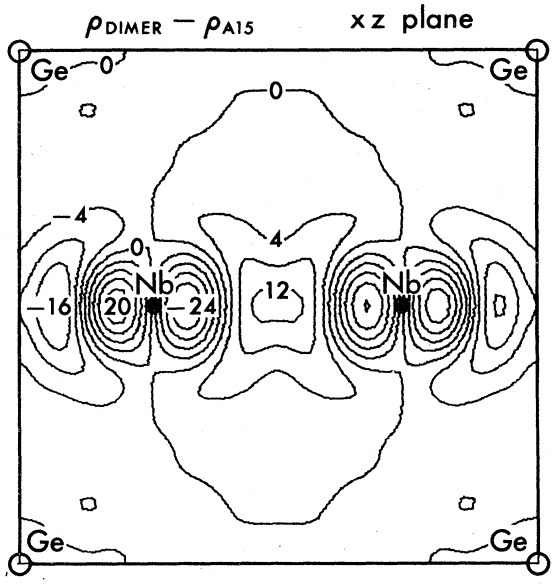

FIG. 12. Difference in the total charge densities of dimerized Nb_3Ge and A-15 Nb_3Ge plotted for the dimerized chain in units of electrons per unit cell.

IV. CONCLUSIONS

Investigations on the electronic charge distributions on several high-T_c A-15 compounds have enabled us to investigate the bonding in these materials. We find that in Nb_3Ge and Nb_3Al, the main charge flow is from the atoms to the interstitial regions contributing to the metallic behavior of the crystal. There are indications of covalent bonding between neighboring Nb atoms on the chain. This characteristic of a mixture of metallic and covalent behavior seems to be the case for a large number of high-T_c compounds as pointed out by Vandenberg and Matthias.[9] Contrary to Bongi's model,[11] we observe no charge transfer from the cubic-site atom to the Nb chains. The effect of the Ge and Al atom on the Nb chain is manifested in a weakening of both the intrachain and interchain coupling, making the crystal more metallic. When the cubic site is occupied by a transition-metal atom (Nb in our case), a bond develops between the cubic-site and the chain-site atom at the expense of the coupling between neighboring atoms on the chain and between neighboring chains. The charge distribution of various states near E_F suggests the importance of states at the R and M points in the electronic instability models of the structural transition in A-15 compounds, whereas previous models[21,22,28] following Gor'kov have focused attention on the X point only. A calculation of the effect of chain dimerization substantiated these conclusions.

TABLE II. Comparison of charge integration results for dimerized Nb_3Ge and undistorted Nb_3Ge. The x chain is the one which is dimerized. The region of integration is a cylinder with axis along the chain and radius $\frac{1}{4}a_c$. Units are electrons per atom.

Undistorted Nb_3Ge		4.09
Dimerized Nb_3Ge:	x chain	4.06
	y chain	4.10
	z chain	4.08

ACKNOWLEDGMENT

This work was supported in part by the Division of Basic Energy Sciences, U.S. Department of Energy and by NSF Grant No. DMR76-20647-A01.

*Present address: Dept. of Physics and Astronomy, Northwestern University, Evanston, Ill. 60201.

[1]W. E. Pickett, K. M. Ko, and M. L. Cohen, preceding paper, Phys. Rev. B 19, 1734 (1979).
[2]L. F. Mattheiss, Phys. Rev. B 12, 2161 (1975); B. M. Klein, L. L. Boyer, and D. A. Papaconstantopoulos, Ferroelectrics 16, 299 (1977); A. T. van Kessel, H. W. Myron, and F. M. Mueller, Phys. Rev. Lett. 41, 181 (1978).
[3]T. Jarlborg and G. Arbman, J. Phys. F 7, 1635 (1977).
[4]S. G. Louie, K. M. Ho, and M. L. Cohen (unpublished).
[5]J. L. Staudenmann, P. Coppens, and J. Muller, Solid State Commun. 19, 29 (1976).
[6]See review articles by L. R. Testardi, in *Physical Acoustics*, edited by W. P. Mason and R. N. Thurston (Academic, New York, 1973), Vol. X, p. 193; M. Weger and I. B. Goldberg, in *Solid State Physics*, edited by H. Ehrenreich, F. Seitz, and D. Turnbull (Academic, New York, 1973), Vol. 28, p. 2.
[7]G. S. Knapp, S. D. Bader, H. V. Culbert, F. Y. Fradin, and T. E. Klippert, Phys. Rev. B 11, 4331 (1975); G. R. Stewart, L. R. Newkirk, and F. A. Valencia, Solid State Commun. 26, 417 (1978); for more references see review articles in Ref. 6.
[8]W. Hanke, J. Hafner, and H. Bilz, Phys. Rev. Lett. 37, 1560 (1976).
[9]J. M. Vandenberg and B. T. Matthias, Science 198, 194 (1977).
[10]R. A. Pollak, C. C. Tsuei, and R. W. Johnson, Solid State Commun. 23, 879 (1977); C. C. Tsuei, S. von Molnar, and J. M. Coey, Phys. Rev. Lett. 41, 664 (1978).

[11]G. H. Bongi, J. Phys. F 6, 1535 (1976).
[12]P. B. Allen, Phys. Rev. B 16, 5139 (1977).
[13]B. W. Batterman and C. S. Barrett, Phys. Rev. Lett. 13, 390 (1964); Phys. Rev. 145, 296 (1966).
[14]R. Mailfert, B. W. Batterman, and J. J. Hanak, Phys. Lett. A 24, 315 (1967); Phys. Status Solidi 32, K67 (1969).
[15]B. N. Kodess, V. B. Kurithzin, and B. N. Tretjakov, Phys. Lett. A 37, 415 (1971); B. N. Kodess, Solid State Commun. 16, 269 (1975).
[16]E. Nembach, K. Tachikawa, and S. Takano, Philos. Mag. 21, 869 (1970).
[17]R. Viswanathan, C. T. Wu, H. L. Luo, and G. W. Webb, Solid State Commun. 14, 1051 (1974).
[18]P. H. Schmidt, E. G. Spencer, D. C. Joy, and J. M. Rowell, in *Superconductivity in d- and f-band Metals*, Second Rochester Conference Proceedings, edited by D. H. Douglass (Plenum, New York, 1976), p. 431.
[19]G. Shirane and J. D. Axe, Phys. Rev. B 4, 2957 (1971).
[20]J. Labbé, S. Barisić, and J. Friedel, Phys. Rev. Lett. 19, 1039 (1967); J. Labbé, Phys. Rev. 172, 451 (1968).
[21]L. P. Gor'kov, Zh. Eksp. Teor. Fiz. Pis'ma Red. 17, 525 (1973) [JETP Lett. 17, 379 (1973)]; Zh. Eksp. Teor. Fiz. 65, 1658 (1973) [Sov. Phys. JETP 38, 830 (1974)].
[22]R. N. Bhatt and W. L. McMillan, Phys. Rev. B 14, 1007 (1976).
[23]R. N. Bhatt, Phys. Rev. B 16, 1915 (1977).
[24]M. V. Jarić and J. L. Birman, Phys. Rev. B 16, 2564 (1977).
[25]S. G. Louie, Phys. Rev. Lett. 40, 1525 (1978); G. P. Kerker, K. M. Ho, and M. L. Cohen, Phys. Rev. Lett. 40, 1593 (1978).
[26]A. R. Miedema, J. Phys. F 4, 120 (1974).
[27]L. J. Vieland and A. W. Wicklund, Phys. Lett. A 49, 407 (1974); S. Mochlecke, D. E. Cox, and A. R. Sweedler, Solid State Commun. 23, 703 (1977).
[28]L. P. Gor'kov and O. N. Dorokhov, J. Low Temp. Phys. 22, 1 (1976); G. Bilbro and W. L. McMillan, Phys. Rev. B 14, 1887 (1976).
[29]T. K. Lee, J. L. Birman, and S. J. Williamson, Phys. Rev. Lett. 39, 839 (1977).